

---

# DAVIS: High-Quality Audio-Visual Separation with Generative Diffusion Models

---

**Chao Huang**  
University of Rochester

**Susan Liang**  
University of Rochester

**Yapeng Tian**  
University of Texas at Dallas

**Anurag Kumar**  
Meta Reality Labs Research

**Chenliang Xu**  
University of Rochester

## Abstract

We propose DAVIS, a **Diffusion model-based Audio-VI**usal Separation framework that solves the audio-visual sound source separation task through a generative manner. While existing discriminative methods that perform mask regression have made remarkable progress in this field, they face limitations in capturing the complex data distribution required for high-quality separation of sounds from diverse categories. In contrast, DAVIS leverages a generative diffusion model and a Separation U-Net to synthesize separated magnitudes starting from Gaussian noises, conditioned on both the audio mixture and the visual footage. With its generative objective, DAVIS is better suited to achieving the goal of high-quality sound separation across diverse categories. We compare DAVIS to existing state-of-the-art discriminative audio-visual separation methods on the domain-specific MUSIC dataset and the open-domain AVE dataset, and results show that DAVIS outperforms other methods in separation quality, demonstrating the advantages of our framework for tackling the audio-visual source separation task.

## 1 Introduction

Visually-guided sound source separation, also referred to as audio-visual separation, is a pivotal task for assessing a machine perception system’s ability to integrate multisensory signals. The primary goal is to isolate individual sounds from a complex audio mixture by utilizing visual cues about the objects that are producing the sounds, e.g., separate the “barking” sound from the mixture by querying the “dog” object. To achieve human-like intelligence, an effective separation model should be capable of handling a *diverse* range of sounds and produce *high-quality* separations that can deliver a realistic auditory experience.

The community has dedicated significant efforts to this task, and existing methods [1–5] have made extensive attempts to tackle this problem, such as developing more powerful separation frameworks [1, 2, 4], proposing more effective training pipeline [5], and incorporating additional visual cues [3] to enhance the separation performance. For optimization, these approaches usually take mask regression [1] or spectrogram reconstruction [6] as training objectives.

While these methods have shown promising separation performance in specific domains, such as musical instrument sounds, they are not yet satisfactory in dealing with open-domain sounds where background noise and off-screen sounds are prevalent. These sounds produce complicated mosaic of time and frequency patterns, posing a significant challenge in achieving high-quality separation. Thus, a natural question arises: *is there an effective approach to model these complex audio data distribution and produce high-quality separated sounds?*

We answer the question by introducing a generative framework for the audio-visual separation. A new class of generative models called denoising diffusion probabilistic models (DDPMs) [7–9], also known as diffusion models, has emerged recently and demonstrated remarkable abilities in generating diverse and high-quality images [10] and audio [11]. The impressive capabilities of generative diffusion models in capturing complex data distributions inspire us to explore their potential for enhancing audio-visual separation. Unlike discriminative modeling, we believe that generative diffusion models can effectively approximate more intricate data distributions, allowing us to handle open-domain time and frequency patterns and lead to superior separation results.

To this end, we present DAVIS, a novel framework for audio-visual separation that is built upon a generative diffusion model. Unlike typical discriminative methods that predict a mask representing the separated sound from the input mixture, DAVIS approaches the separation task as a conditional generation process. Specifically, our method incorporates a T-step diffusion and reverse process [7, 10, 8]: during the training stage, Gaussian noise controlled by a variance schedule [12] is added to the unmixed sound at each diffusion step. In the reverse process, our method initiates from a standard Gaussian distribution, and an effective Separation U-Net is proposed to estimate the noise added at each diffusion step, iteratively generating the separated magnitude with guidance from the mixture and visual footage. The Separation U-Net comprises an encoder-decoder structure with enabled skip connections. To capture both local time-frequency patterns and long-range time dependencies, we introduce a CA block consisting of two ResNet blocks for capturing local patterns and a Time-Attention block for learning long-range time correlation. Furthermore, to enhance audio-visual association learning, we devise a Feature Interaction module to facilitate interactions between audio and visual features and inject visual cues into the separation.

Experiments on the MUSIC [1] and AVE [13] datasets demonstrate that DAVIS outperforms the state-of-the-art methods in terms of separation quality. Our contributions are summarized as follows:

- We are the first study, to the best of our knowledge, to approach the audio-visual separation task as a conditional generation process and solve it using a diffusion model.
- We design a Separation U-Net, which incorporates CA blocks and a Feature Interaction module to capture the audio-visual association effectively.
- Our framework surpasses previous methods on both specific and open-domain sound datasets, highlighting the benefits of solving audio-visual separation through a generative approach.

## 2 Related Work

**Audio-Visual Sound Source Separation.** In this section, our focus is on modern audio-visual sound source separation approaches while acknowledging the prolonged research efforts dedicated to sound source separation in signal processing. Recent deep learning-based audio-visual sound source separation methods have been applied to different categories of audio, such as speech signals [14, 6, 15, 16], musical instrument sounds [1, 3, 5, 2, 17, 4], and universal sound sources [18–23]. These methods typically employ a learning regime that involves mixing two audio streams from different videos to provide supervised training signals. A sound separation network, often implemented as a U-Net, is then used for mask regression [1, 2, 5, 24] conditioned on associated visual representations. In recent years, research in this area has shifted from solving domain-specific sound source separation to addressing the challenge of open-domain sounds [20, 21, 19]. However, such methods require text-query [20] or estimating motion information [19]. In this paper, we propose a novel audio-visual separation approach that can handle both specific and open-domain sound sources.

**Diffusion Models.** Diffusion models [7, 25, 26] fall under the category of deep generative models that start with a sample in a random distribution and gradually restore the data sample through a denoising process. Recently, diffusion models have exhibited remarkable performance across various domains, including computer vision [10, 27–34], natural language processing [35–38], and audio applications [11, 39, 40, 38, 41–43]. While diffusion models have been successfully employed for single-modality generation, their potential for audio-visual tasks remains largely unexplored. For instance, only recently has MM-diffusion [44] proposed simultaneous generation of videos and audio. Furthermore, there has been a growing interest in employing diffusion models for discriminative tasks. Some pioneer works have explored the application of diffusion models to image segmentation [45–47] and object detection [48]. However, despite significant interest in this direction, there have been no prior successful attempts to apply generative diffusion models to audio-visual scene understanding, which has notably lagged behind the progress in visual perception tasks. To the best of our knowledge,

this paper presents the first work that adopts a diffusion model to learn audio-visual associations for audio-visual sound source separation.

### 3 Method

In this section, we introduce DAVIS, our novel diffusion model-based audio-visual separation framework designed for achieving high-quality separation results. We begin by providing a brief recap of the preliminary knowledge of diffusion models in Sec. 3.1. Next, we present our proposed Separation U-Net architecture, which effectively captures the audio-visual association through the generation process in Sec. 3.3. Finally, we discuss the training and inference designs in Sec. 3.4 and Sec. 3.5, respectively.

#### 3.1 Preliminaries

We introduce the concept of diffusion models, which serves to illustrate the pipeline of our framework. A diffusion model consists of a forward and a reverse process. The forward process is defined as a Markovian chain that gradually adds noise to the data sample  $x_0$  according to a variance schedule  $\beta_1, \dots, \beta_T$ :

$$q(x_{1:T}|x_0) = \prod_{i=1}^T q(x_i|x_{i-1}), \quad (1)$$

$$q(x_t|x_{t-1}) = \mathcal{N}(x_t|\sqrt{\bar{\alpha}_t}x_{t-1}, \beta_t\mathbf{I}), \quad (2)$$

where  $\alpha_t = 1 - \beta_t$  and  $\bar{\alpha}_t = \prod_{s=0}^t \alpha_s$ . Note that the variance schedule is also fixed during the reverse process. If the total number of  $T$  goes to infinity, the diffusion process will finally lead to pure noise, *i.e.*, the distribution of  $p(x_T)$  is  $\mathcal{N}(x_T; \mathbf{0}, \mathbf{I})$  with only Gaussian noise.

The reverse process aims to recover samples from Gaussian distribution by removing the noise gradually, which is a Markovian chain parameterized by  $\theta$ :

$$p_\theta(x_{0:T}) = p_\theta(x_T) \prod_{t=1}^T p_\theta(x_{t-1}|x_t), \quad (3)$$

where at each iteration, the noise  $\epsilon$  added in the forward process is estimated as:

$$p_\theta(x_{t-1}|x_t) = \mathcal{N}(x_{t-1}; \boldsymbol{\mu}_\theta(x_t, t), \boldsymbol{\Sigma}_\theta(x_t, t)). \quad (4)$$

Note that we set the variances  $\boldsymbol{\Sigma}_\theta(x_t, t) = \tilde{\beta}_t\mathbf{I}$  to untrained constants and  $\boldsymbol{\mu}_\theta(x_t, t)$  is usually implemented as neural networks. To adapt the diffusion process into a conditional one, we include the conditional context  $\mathbf{c}$  as additional network inputs, which modifies Eq. 4 as follows:

$$p_\theta(x_{t-1}|x_t) = \mathcal{N}(x_{t-1}; \boldsymbol{\mu}_\theta(x_t, t, \mathbf{c}), \tilde{\beta}_t\mathbf{I}), \quad \text{where } \tilde{\beta}_t := \frac{1 - \bar{\alpha}_{t-1}}{1 - \bar{\alpha}_t} \beta_t. \quad (5)$$

We follow [7] to use a simplified training objective:

$$L_{simple}(\theta) = \mathbb{E}_{t, x_0, \epsilon} [|\epsilon - \epsilon_\theta(\sqrt{\bar{\alpha}_t}x_0 + \sqrt{1 - \bar{\alpha}_t}\epsilon, \mathbf{c}, t)|], \quad (6)$$

where  $\epsilon_\theta$  represents a function approximator used to predict  $\epsilon$ , while  $t$  denotes a uniformly sampled value ranging from 1 to  $T$ . The loss function computes a weighted variational bound that highlights different aspects of the reconstruction.

#### 3.2 Task Setup and Method Overview

Given an unlabeled video clip  $V$ , we can extract an audio-visual pair  $(a, v)$ , where  $a$  and  $v$  denote the audio and visual stream, respectively. In real-world scenarios, the audio stream can be a mixture of  $N$  individual sound sources, denoted as  $a = \sum_{i=1}^N s_i$ , where each source  $s_i$  can be of various categories. The primary goal of the visually-guided sound source separation task is to utilize visual cues from  $v$  to effectively separate  $a$  into its constituent sources  $s_i$ , for  $i \in \{1, 2, \dots, N\}$ . Since no labels are provided to distinguish the sound sources  $s_i$ , prior works [1, 5, 24] have commonly used a ‘‘mix and

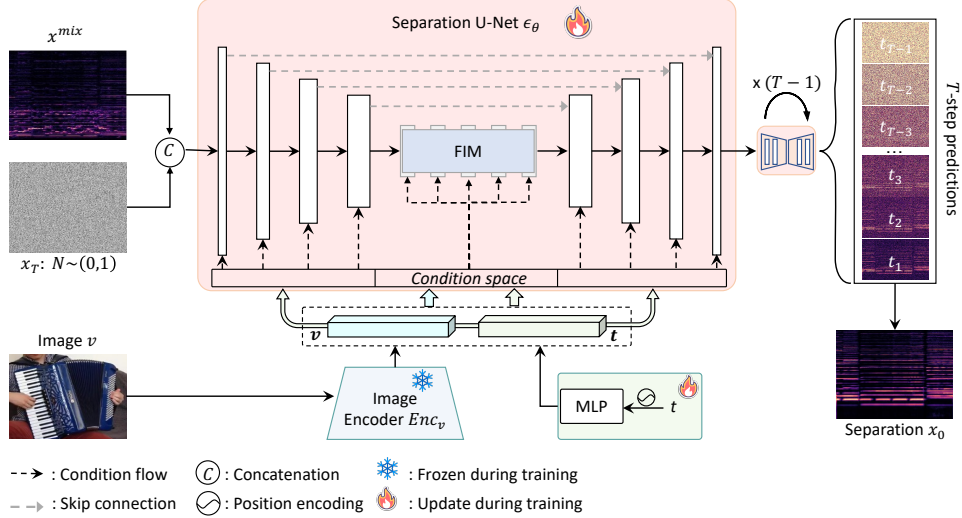


Figure 1: **Overview of the DAVIS framework.** Our objective is to synthesize the separated sound  $x_0$  by leveraging an audio mixture  $x^{mix}$  and an image  $v$ , while taking into account the diffusion timestep  $t$ . Firstly, we sample a latent variable  $x_T$  from a standard distribution. Next, we encode the image  $v$  and the timestep  $t$  into the embedding space, resulting in feature vectors  $v$  and  $t$ . These features serve as conditions in the Separation U-Net  $\epsilon_\theta$ , which performs iterative denoising on  $x_T$  to obtain the separated sound  $x_0$ . Specifically,  $t$  is passed to all the modules within  $\epsilon_\theta$ , while  $v$  is only utilized in the Feature Interaction Module (Sec. 3.3) to enhance audio-visual association learning.

separate” strategy, which involves mixing audio streams from two different videos and manually create the mixture:  $a^{mix} = a^{(1)} + a^{(2)}$ . Furthermore, the time series  $a$  is usually transformed into magnitude spectrogram by short-time Fourier transform (STFT):  $x = \text{STFT}(a) \in \mathbb{R}^{T \times F}$ , allowing for manipulations in the 2D-like Time-Frequency domain, where  $F$  and  $T$  are the numbers of frequency bins and time frames, respectively. Consequently, the goal of training is to learn a separation network capable of mapping  $(x^{mix}, v^{(1)}) \rightarrow x^{(1)}$ . For simplicity, we will omit the video index notation in the subsequent sections<sup>1</sup>.

In contrast to discriminative approaches that perform the mapping through regression, our proposed DAVIS framework is built on a diffusion model with a T-step diffusion and reverse process. The diffusion process is determined by a fixed variance schedule as described in Eq. (1) and Eq. (2), which gradually adds noises to the magnitude spectrogram  $x_0$  and converts it to latent  $x_T$ . As depicted in Fig. 1, the reverse process (according to Eq. (3) and Eq. (5)) of DAVIS is specified by our proposed separation network  $\epsilon_\theta$ . This reverse process iteratively denoises a latent variable  $x_T$ , which is sampled from a uniform distribution, to obtain a separated magnitude conditioned on the magnitude of the input sound mixture  $x^{mix}$  and the visual footage  $v$ . Consequently, the objective of the separation network  $\epsilon_\theta$  is to predict the noise  $\epsilon$  added at each diffusion timestep during the forward process.

### 3.3 Separation U-Net

Previous works [2, 4] often utilize a U-Net [49]-like architecture for separation network designs. This choice is attributed to the U-Net’s effectiveness in capturing multi-level feature representations and producing separated magnitudes with the same shape as inputs. Exploiting the grid-like nature of magnitude spectrograms, existing methods employ convolution-based U-Nets for separation and concatenate audio and visual features directly at the bottleneck to incorporate visual cues. While these approaches achieve good separation performance, we argue that they may be inadequate for real-world sound mixtures due to two key reasons. Firstly, similar frequency patterns can occur in temporally distant frames, and distinct frequency patterns can mix within a single time frame. Such occurrences necessitate the network to capture both local patterns and long-range dependencies across time and frequency dimensions, where pure convolution may fall short. Motivated by this, we propose a novel Separation U-Net (depicted in Fig. 1) that incorporates Convolution-Attention (CA) blocks

<sup>1</sup>In this paper, superscripts denote video indices, while subscripts refer to diffusion timesteps.

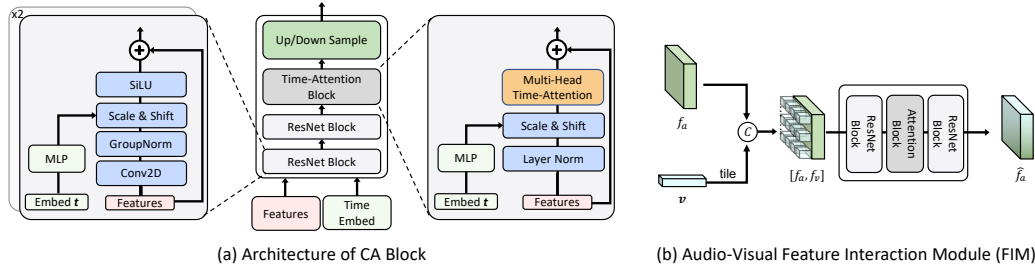


Figure 2: **Illustrations on CA Block and Feature Interaction Module.** (a) Our CA block operates by taking audio feature maps and a time embedding  $t$  as inputs. Each sub-block, except the up/down sampling layer, is conditioned on  $t$ . It consists of two groups of convolutions within each ResNet block to capture local time-frequency patterns, while the Time-Attention block captures long-range dependencies along the time dimension. (b) The Feature Interaction Module functions by replicating and concatenating  $v$  with  $f_a$ . Two identical ResNet blocks, as described in (a), are used to process the concatenated features. However, in contrast to (a), the attention block here operates on both the frequency and time dimensions instead of solely aggregating temporal contexts.

(elaborated in Fig. 2). These blocks combine sequential convolution and time-attention mechanisms to learn both local and global time-frequency associations. Secondly, learning representative audio-visual associations is crucial for the task. While existing methods directly concatenate visual features and audio embeddings at the bottleneck and feed them to the decoder network for mask regression, such approaches lack the ability to foster further interactions between audio and visual features. To address this limitation, we introduce an audio-visual feature interaction module, which enhances association learning by enabling interactions between audio and visual modalities.

**Timestep Embedding.** In a diffusion model, the timestep embedding serves to inform the model about the current position of the input within the Markovian chain. As shown in Fig. 1, diffusion time  $t$  is specified by the Transformer sinusoidal position embedding [50] and further transformed by an MLP, which will be passed to each CA block as a condition.

**Encoder/Decoder Designs.** Our proposed Separation U-Net architecture comprises an encoder and a decoder, with an audio-visual feature interaction module in between. Both the encoder and decoder consist of four CA Blocks, and skip connections are utilized to facilitate information flow. Initially, we concatenate the latent variable  $x_T$  with the mixture  $x^{mix}$  along the channel dimension and employ a  $1 \times 1$  convolution to project it to the feature space. As depicted in Fig. 2, each CA block in the encoder consists of two ResNet blocks for extracting local time-frequency patterns and one Time-Attention block for capturing long-range time dependencies. Following this, a downsample layer (or upsample layer for the decoder) with a scale factor of 2 is used. Specifically, we construct the ResNet block using WeightStandardized 2D convolution [51] along with GroupNormalization [52] and SiLU activation [53]. To incorporate the time embedding  $t$  as a conditioning factor, we employ an MLP to generate  $t$ -dependent scaling and shifting vectors for feature-wise affine transformation [54] before the activation layer. A Time-Attention block is appended after the ResNet blocks to capture long-range time dependencies. For implementation, we adopt the design proposed by Wang et al. [55], which includes Pre-Layer Normalization and Multi-Head Attention along the time dimension within the residual connection. The downscale and upscale layers are implemented using 2D convolutions with a stride of 2. As a result, we can obtain audio feature maps  $f_a \in \mathbb{R}^{C \times \frac{T}{16} \times \frac{F}{16}}$  at the bottleneck, where  $C$  represents the number of channels. Additionally, we include a  $1 \times 1$  convolution to convert the decoder output into magnitude.

**Audio-Visual Feature Interaction Module.** The key to achieving successful audio-visual separation lies in effectively utilizing visual information to separate visually-indicated sound sources. Therefore, the interaction between audio and visual modalities at the feature level becomes crucial. Existing approaches typically concatenate audio and visual features at the bottleneck [2, 4] and pass them to the decoder for further fusion. In this paper, we propose a novel audio-visual feature interaction module to enhance this capability. Concretely, given the visual footage  $v$ , we first use a pre-trained ResNet-18 [56] visual backbone  $\mathbf{Enc}_v$  to extract the global embedding  $v := \mathbf{Enc}_v(v) \in \mathbb{R}^C$ . Since the number of channels in the visual embedding  $v$  matches that of  $f_a$ , we can omit the modality notation. Next, we tile  $v$  to match the shape of  $f_a$ , resulting in visual feature maps  $f_v$ . Subsequently,

the audio and visual feature maps are concatenated and fed into the feature interaction module (FIM):  $\hat{\mathbf{f}}_a := \mathbf{FIM}([\mathbf{f}_a, \mathbf{f}_v])$ , where  $\hat{\mathbf{f}}_a \in \mathbb{R}^{C \times \frac{T}{16} \times \frac{F}{16}}$ . The details of the FIM module are illustrated in Fig. 2(b), encompassing ResNet blocks and a time-frequency attention block that facilitate the establishment of audio-visual associations in both local and global regions.

### 3.4 Training

---

#### Algorithm 1 Training

---

- 1: **Input:** A dataset  $D$  that contains audio-visual pairs  $\{(a^{(k)}, v^{(k)})\}_{k=1}^K$ , total diffusion step  $T$
  - 2: **Initialize:** randomly initialize Separation U-Net  $\epsilon_\theta$  and pre-trained visual encoder  $\mathbf{Enc}_v$
  - 3: **repeat**
  - 4:   Sample  $(a^{(1)}, v^{(1)})$  and  $(a^{(2)}, v^{(2)}) \sim D$
  - 5:   Mix and compute  $x^{mix}, x^{(1)}$
  - 6:   Scale  $x = \log_e(1 + x) \cdot \sigma$  and clip  $x^{mix}, x^{(1)}$  to  $[0, 1]$
  - 7:   Encode visual frame  $v^{(1)}$  as  $\mathbf{v}^{(1)} := \mathbf{Enc}_v(v^{(1)})$
  - 8:   Sample  $\epsilon \sim \mathcal{N}(\mathbf{0}, \mathbf{I})$ , and  $t \sim \text{Uniform}(1, \dots, T)$
  - 9:   Take gradient step on
  - 10:    $\nabla_\theta \|\epsilon - \epsilon_\theta(x_t^{(1)}, x^{mix}, \mathbf{v}^{(1)}, t)\|, x_t^{(1)} = \sqrt{\bar{\alpha}_t}x^{(1)} + \sqrt{1 - \bar{\alpha}_t}\epsilon$
  - 11: **until** converged
- 

Algorithm 1 depicts the complete training procedure of our DAVIS framework. Given the sampled audio-visual pairs from the dataset, we first adopt the ‘‘mix and separate’’ strategy and compute the magnitudes  $x^{(1)}, x^{(2)}, x^{mix}$  with STFT.

**Data Scaling:** To align with the frequency decomposition of the human auditory system, we apply a logarithmic transformation to the magnitude spectrogram, converting it to a log-frequency scale. Additionally, we ensure consistent scaling of the log-frequency magnitudes by multiplying them with a scale factor  $\sigma$  and clipping the values to fall within the range  $[0, 1]$ .

The visual frames are encoded to embeddings  $\mathbf{v}^{(1)}, \mathbf{v}^{(2)}$ . Taking video (1) as an example, we sample  $\epsilon$  from a standard Gaussian distribution and  $t$  from the set  $\{1, \dots, T\}$ . Then, we input  $x_t^{(1)}, x^{mix}, \mathbf{v}^{(1)}, t$  to the Separation U-Net  $\epsilon_\theta$  and optimize the network by taking a gradient step on Eq. (6). In practice, we use both video (1) and (2) for optimization, therefore the final loss term is formulated as  $\mathcal{L} = \mathcal{L}_{simple}^{(1)}(\theta) + \mathcal{L}_{simple}^{(2)}(\theta)$ .

### 3.5 Inference

---

#### Algorithm 2 Inference

---

- 1: **Input:** Audio mixture  $a^{mix}$  and the query visual frame  $v$ , total diffusion step  $T$
  - 2: Sample  $x_T \sim \mathcal{N}(\mathbf{0}, \mathbf{I})$
  - 3: Compute  $x^{mix} := \mathbf{STFT}(a^{mix})$
  - 4: Encode visual frame  $v := \mathbf{Enc}_v(v)$
  - 5: **for**  $t = T, \dots, 1$  **do**
  - 6:   Sample  $z \sim \mathcal{N}(\mathbf{0}, \mathbf{I})$  if  $t > 1$ , else  $z = 0$
  - 7:   Compute  $x_{t-1}: x_{t-1} = \frac{1}{\sqrt{\alpha_t}}(x_t - \frac{1-\alpha_t}{\sqrt{1-\alpha_t}}\epsilon_\theta(x_t, x^{mix}, \mathbf{v}, t)) + \sqrt{\tilde{\beta}_t}z$
  - 8: **end for**
  - 9: **return**  $e^{x_0/\sigma} - 1$
- 

As illustrated in Algorithm 2, our inference process starts from a sampled latent variable  $x_T$ , and takes the mixture  $x^{mix}$  and visual frame embedding  $\mathbf{v}$  as conditions to produce the separated magnitude  $x_0$  through  $T$  iterations. Finally, the output is rescaled to the original value range.

Methods	Output	MUSIC [1]			AVE [13]		
		SDR	SIR	SAR	SDR	SIR	SAR
SoP [1]	Mask	3.42	4.98	-	0.46	4.17	12.08
CoSep [2]	Mask	2.04	6.21	-	-1.33	2.54	5.77
CCoL [5]	Mask	7.18	12.55	11.09	1.77	3.25	22.52
DAVIS	Mag.	9.29	14.19	15.76	1.78	6.61	7.76

Table 1: Comparisons with different discriminative audio-visual separation approaches on MUSIC and AVE test sets. The “Output” category highlights the distinction between our method (magnitude synthesis) and others (mask regression). We report SDR, SIR, and SAR metrics and mark our results in gray. Note that numbers marked in red actually indicate poor performance (Sec. 4.2).

## 4 Experiments

### 4.1 Experimental Setup

**Datasets.**<sup>2</sup> Our model demonstrates the ability to handle both specific and open-domain sound separation. To evaluate our approach, we use MUSIC [1] and AVE [13] datasets, which cover musical instruments and open-domain sounds. The evaluation settings are described in detail below:

- **MUSIC:** We evaluate our proposed method on the widely-used MUSIC [1] dataset, which includes 11 musical instrument categories: accordion, acoustic guitar, cello, clarinet, erhu, flute, saxophone, trumpet, tuba, violin, and xylophone. All the videos are clean solo and the sounding instruments are usually visible. We follow CCoL [5] and use the same train/val/test splits, resulting in a total of 468/26/26 videos across various instrument categories.
- **AVE:** In addition to the MUSIC dataset, we also evaluate our method on the Audio-Visual Event (AVE) dataset [13]. This dataset contains 4143 10-second videos, including 28 diverse sound categories, such as *Church Bell*, *Barking*, and *Frying (Food)*, among others. The AVE dataset presents greater challenges as the audio in these videos may not span the entire duration and can be noisy, including off-screen sounds (e.g., human speech) and background noise. We conduct training and evaluation on this demanding dataset using the original train/val/test splits, consisting of 3339/402/402 videos, respectively.

**Baselines.** To the best of our knowledge, we are the first to adopt a generative model for the audio-visual source separation task. Thus, we compare DAVIS against the following state-of-the-art discriminative methods: (i) *Sound of Pixels* (SoP) [1] that learns ratio mask predictions with a 1-frame-based model, (ii) *Co-Separation* (CoSep) [2] that takes a single visual object as the condition to perform mask regression, (iii) *Cyclic Co-Learn* (CCoL) [5] which jointly trains the model with sounding object visual grounding and visually-guided sound source separation tasks. Since the AVE dataset lacks bounding box annotation for detected objects, we use the entire image for CoSep and CCoL. For all the comparative methods, we use the authors’ publicly available code. Several other recent works [22, 57] have achieved impressive separation results. However, due to the unavailability of their source code, we will not include them in our comparative analysis.

**Evaluation Metrics.** To quantitatively evaluate the audio-visual sound source separation performances, we use the standard metrics [1, 5, 2], namely: Signal-to-Distortion Ratio (SDR), Signal-to-Interference Ratio (SIR), and Signal-to-Artifact Ratio (SAR). We adopt the widely-used mir eval library [58] to report the standard metrics. Note that SDR and SIR evaluate the accuracy of source separation, whereas SAR specifically measures the absence of artifacts [2]. Consequently, SAR can be high even if the separation performance is poor in terms of accurately separating the sources.

**Implementation Details.** In our experimental setup, we down-sample audio signals at 11kHz, and the video frame rate is set to 1 fps. For the MUSIC dataset, each video is approximately 6 seconds and we randomly select 3 frames per video. As for the AVE dataset, we use the entire 10-second audio as input and only select 1 frame that falls into the audio-visual event boundary [13] for training the model. This selection ensures that the auditory object occurs within the visual frame, facilitating audio-visual association learning. During training, the frames are first resized to  $256 \times 256$  and then randomly cropped to  $224 \times 224$ . We set the total time step  $T = 1000$  to train our DAVIS

<sup>2</sup>All collection, processing, and use of data obtained from datasets was conducted by the University of Rochester.



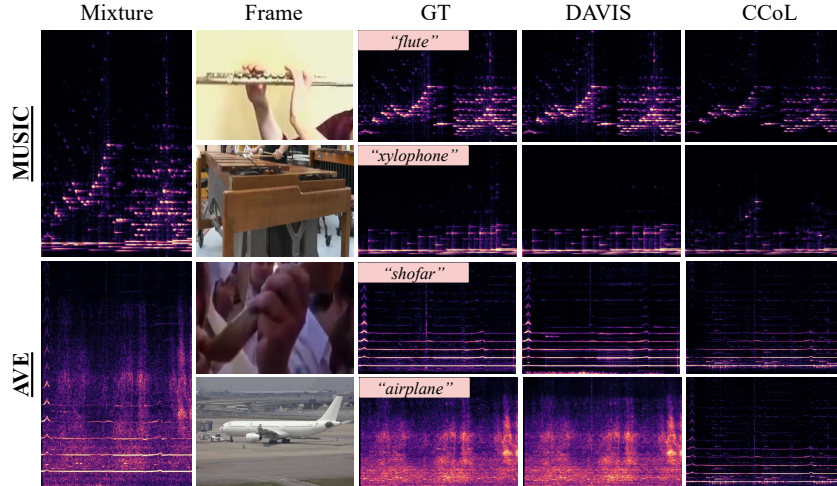


Figure 3: Visualizations of audio-visual separation results on the MUSIC (top) and AVE (bottom) datasets. Two sounds are mixed (mixture), and referenced frames are provided to guide the separation. We show the comparison between ground truth spectrograms and DAVIS/CCoL’s predictions.

model. During inference, all the frames are directly resized to the desired size without cropping. To accelerate the separation process, we use DDIM [9] with a sampling step of 25. The audio waveform is transformed into a spectrogram with a Hann window of size 1022 and a hop length of 256. The obtained magnitude spectrogram is subsequently resampled to  $256 \times 256$  to feed into the separation network. We set the number of audio and visual feature channels  $C$  as 512 and empirically choose the scale factor  $\sigma = 0.15$ . Our model is trained with the Adam optimizer, with a learning rate of  $10^{-4}$ . The training is conducted on a single A6000 GPU for 200 epochs with a batch size of 10.

## 4.2 Comparisons with State-of-the-art

To evaluate the effectiveness of our method, we present separation results by comparing DAVIS with state-of-the-art approaches on the MUSIC and AVE datasets, as depicted in Tab. 1. Indeed, SDR is a reliable metric for measuring source separation accuracy in clean datasets like MUSIC, as it does not consider interference. On the other hand, SIR is useful for evaluating source separation in multi-source scenarios, which is suitable for open-domain datasets like AVE. Our results highlight the advantages of utilizing generative modeling for audio-visual separation. DAVIS consistently outperforms previous approaches across various evaluation categories, achieving up to a 2.1 dB improvement on the SDR scale for the MUSIC dataset and a 3.4 dB improvement on the SIR scale for the AVE dataset, surpassing the performance of the next best approach CCoL. These results clearly demonstrate the versatility of our method across diverse datasets with varying visual and audio contexts. Among the competing techniques, we observe that CCoL and SoP yield higher SAR results than our method on the AVE dataset. However, we argue that high SAR values do not necessarily imply effectiveness, as they can arise from poor separation. It is worth noting that a comparison between the mixture spectrogram and the ground truth unmixed spectrogram can surprisingly yield high SAR values. In this context, we believe that our method significantly improves separation performance compared to others. In Fig. 3, we visually compare our separation results to the CCoL baseline. Our visualizations demonstrate that DAVIS achieves higher separation quality, as evidenced by the closer resemblance of our separated magnitude spectrograms to the ground truth. Moreover, the successful handling of diverse time patterns in the provided examples highlights the importance of incorporating time-attention mechanisms in DAVIS.

## 4.3 Experimental Analysis

**Ablation Study.** We conduct ablation experiments on the MUSIC validation set to examine the different components of DAVIS. Firstly, we validate the effectiveness of our proposed CA block by designing two baselines: (a) replacing the Time-Attention mechanism within the CA block with a ResNet block (shown in Fig. 2 (a)), which only captures local time-frequency patterns, and (b)



employing a Time-Frequency Attention mechanism that calculates attention weights along both the time and frequency dimensions. To ensure a fair comparison, we adopt an efficient attention mechanism [59] to mitigate computational overhead, resulting in a similar computation cost as our Time-Attention block. The results presented in Tab. 2 demonstrate the significance of capturing long-range time dependencies, while our Time-Attention mechanism achieves a favorable trade-off between computation and performance compared to Time-Frequency attention. Second, in Tab. 3, we investigate the impact of varying the number of sampling steps. We observe that setting the step value to 25 yields the best results in our setting. Meanwhile, even with step = 10, satisfactory results are obtained, indicating the potential for further acceleration if faster inference speed is prioritized.

Methods	SDR	SIR	SAR
ResNet Block	4.90	10.21	9.65
Time Attn.	7.57	12.55	15.50
Time-Freq Attn.	7.39	14.03	12.63

Table 2: Ablation on CA block design.

Sampling step	SDR	SIR	SAR
Step=10	7.03	11.48	15.45
Step=15	7.29	11.95	15.56
Step=25	7.57	12.55	15.50
Step=50	7.40	12.61	15.31

Table 3: Number of sampling steps.

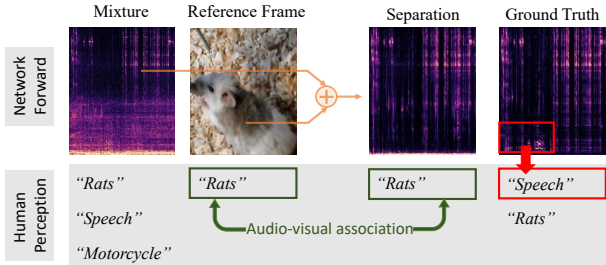


Figure 4: An visualization example showing that our DAVIS model can capture accurate audio-visual association to perform visually-guided separation.

**Learned Audio-Visual Association.** The learned associations between audio and visual features play a crucial role in the success of separation. To demonstrate our learned associations, we present an example from the AVE dataset in Fig. 4. In this example, a video clip labeled “Rats” is mixed with another video clip labeled “Motorcycle.” However, human perception reveals the presence of an off-screen sound “Speech.” occurring in the “Rats” clip, while only the “rat” object is visible in the reference frame. In this scenario, our method successfully separates the “Rats” sound from the complicated mixture while disregarding the “Speech,” thus affirming the accuracy of our learned audio-visual associations and our method’s capability to capture complex data distribution.

## 5 Limitation and Discussion

Our proposed DAVIS framework incorporates the extraction of global visual embedding as a condition for visually-guided source separation. This technique, which utilizes global visual features, has been widely adopted in audio-visual learning [1, 24]. Unlike methods that rely on pre-trained object detectors for extracting visual features, our framework does not have such a dependency. However, it may encounter limitations when trained on unconstrained video datasets. Intuitively, successful results can be achieved when the video contains a distinct sounding object, such as solo videos in the MUSIC dataset or videos capturing a sounding object performing a specific event in the AVE dataset. Nonetheless, this training assumption may not hold in more challenging scenarios, where multiple objects are likely producing sounds, rendering the global visual embedding inadequate for accurately describing the content of sounding objects. To address this issue, one possible approach is to adapt our framework to leverage more fine-grained visual features and jointly learn sounding object localization and visually-guided sound separation. This adaptation enables the model to utilize localized sounding object information to enhance the audio-visual association.

## 6 Conclusion and Future Work

In this paper, we propose DAVIS, a diffusion model-based audio-visual separation framework designed to address the problem in a generative manner. Unlike approaches relying on discriminative training objectives for regression, our separation framework is built upon a T-step diffusion model, allowing for iterative synthesis of the separated magnitude spectrogram while conditioning on the visual footage. Leveraging the power of generative modeling, our method effectively handles complex data distributions and achieves high-quality sound separation. Extensive experiments on the MUSIC and AVE datasets validate the efficacy of our framework, demonstrating its effectiveness in separating

sounds within specific domains (e.g., music instrument sounds) as well as its ability to generalize to open-domain sound categories.

Our approach initiates the utilization of generative models for audio-visual scene understanding, paving the way for potential extensions to other multi-modal perception tasks like audio-visual object localization. Humans demonstrate the ability to imagine a "dog" upon hearing a "barking" sound, highlighting the potential of cross-modal generation in advancing audio-visual association learning. This implies that localization and separation tasks can be integrated into a single generative framework. In the future, we plan to explore the application of generative models to jointly address audio-visual localization and separation tasks.

## References

- [1] Hang Zhao, Chuang Gan, Andrew Rouditchenko, Carl Vondrick, Josh McDermott, and Antonio Torralba. The sound of pixels. In *Proceedings of the European conference on computer vision (ECCV)*, pages 570–586, 2018.
- [2] Ruohan Gao and Kristen Grauman. Co-separating sounds of visual objects. In *Proceedings of the IEEE/CVF International Conference on Computer Vision*, pages 3879–3888, 2019.
- [3] Chuang Gan, Deng Huang, Hang Zhao, Joshua B Tenenbaum, and Antonio Torralba. Music gesture for visual sound separation. In *Proceedings of the IEEE/CVF Conference on Computer Vision and Pattern Recognition*, pages 10478–10487, 2020.
- [4] Moitrey Chatterjee, Jonathan Le Roux, Narendra Ahuja, and Anoop Cherian. Visual scene graphs for audio source separation. In *Proceedings of the IEEE/CVF International Conference on Computer Vision*, pages 1204–1213, 2021.
- [5] Yapeng Tian, Di Hu, and Chenliang Xu. Cyclic co-learning of sounding object visual grounding and sound separation. In *Proceedings of the IEEE/CVF Conference on Computer Vision and Pattern Recognition*, pages 2745–2754, 2021.
- [6] Andrew Owens and Alexei A Efros. Audio-visual scene analysis with self-supervised multisensory features. In *Proceedings of the European Conference on Computer Vision (ECCV)*, pages 631–648, 2018.
- [7] Jonathan Ho, Ajay Jain, and Pieter Abbeel. Denoising diffusion probabilistic models. *Advances in Neural Information Processing Systems*, 33:6840–6851, 2020.
- [8] Alexander Quinn Nichol and Prafulla Dhariwal. Improved denoising diffusion probabilistic models. In *International Conference on Machine Learning*, pages 8162–8171. PMLR, 2021.
- [9] Jiaming Song, Chenlin Meng, and Stefano Ermon. Denoising diffusion implicit models. *arXiv preprint arXiv:2010.02502*, 2020.
- [10] Prafulla Dhariwal and Alexander Nichol. Diffusion models beat gans on image synthesis. *Advances in Neural Information Processing Systems*, 34:8780–8794, 2021.
- [11] Zhifeng Kong, Wei Ping, Jiaji Huang, Kexin Zhao, and Bryan Catanzaro. Diffwave: A versatile diffusion model for audio synthesis. *arXiv preprint arXiv:2009.09761*, 2020.
- [12] Allan Jabri, David Fleet, and Ting Chen. Scalable adaptive computation for iterative generation. *arXiv preprint arXiv:2212.11972*, 2022.
- [13] Yapeng Tian, Jing Shi, Bochen Li, Zhiyao Duan, and Chenliang Xu. Audio-visual event localization in unconstrained videos. In *Proceedings of the European Conference on Computer Vision (ECCV)*, pages 247–263, 2018.
- [14] Ariel Ephrat, Inbar Mosseri, Oran Lang, Tali Dekel, Kevin Wilson, Avinatan Hassidim, William T Freeman, and Michael Rubinstein. Looking to listen at the cocktail party: A speaker-independent audio-visual model for speech separation. *arXiv preprint arXiv:1804.03619*, 2018.
- [15] Triantafyllos Afouras, Andrew Owens, Joon Son Chung, and Andrew Zisserman. Self-supervised learning of audio-visual objects from video. In *European Conference on Computer Vision*, pages 208–224. Springer, 2020.
- [16] Daniel Michelsanti, Zheng-Hua Tan, Shi-Xiong Zhang, Yong Xu, Meng Yu, Dong Yu, and Jesper Jensen. An overview of deep-learning-based audio-visual speech enhancement and separation. *IEEE/ACM Transactions on Audio, Speech, and Language Processing*, 29:1368–1396, 2021.

- [17] Hang Zhao, Chuang Gan, Wei-Chiu Ma, and Antonio Torralba. The sound of motions. In *Proceedings of the IEEE/CVF International Conference on Computer Vision*, pages 1735–1744, 2019.
- [18] Ruohan Gao, Rogerio Feris, and Kristen Grauman. Learning to separate object sounds by watching unlabeled video. In *Proceedings of the European Conference on Computer Vision (ECCV)*, pages 35–53, 2018.
- [19] Himangi Mittal, Pedro Morgado, Unnat Jain, and Abhinav Gupta. Learning state-aware visual representations from audible interactions. In *Proceedings of the European conference on computer vision (ECCV)*, 2022.
- [20] Hao-Wen Dong, Naoya Takahashi, Yuki Mitsufuji, Julian McAuley, and Taylor Berg-Kirkpatrick. Clipsep: Learning text-queried sound separation with noisy unlabeled videos. *arXiv preprint arXiv:2212.07065*, 2022.
- [21] Efthymios Tzinis, Scott Wisdom, Aren Jansen, Shawn Hershey, Tal Remez, Daniel PW Ellis, and John R Hershey. Into the wild with audioscope: Unsupervised audio-visual separation of on-screen sounds. *arXiv preprint arXiv:2011.01143*, 2020.
- [22] Efthymios Tzinis, Scott Wisdom, Tal Remez, and John R Hershey. Audioscopev2: Audio-visual attention architectures for calibrated open-domain on-screen sound separation. In *Computer Vision—ECCV 2022: 17th European Conference, Tel Aviv, Israel, October 23–27, 2022, Proceedings, Part XXXVII*, pages 368–385. Springer, 2022.
- [23] Moitreya Chatterjee, Narendra Ahuja, and Anoop Cherian. Learning audio-visual dynamics using scene graphs for audio source separation. In *NeurIPS*, 2022.
- [24] Chao Huang, Yapeng Tian, Anurag Kumar, and Chenliang Xu. Egocentric audio-visual object localization. *arXiv preprint arXiv:2303.13471*, 2023.
- [25] Yang Song, Jascha Sohl-Dickstein, Diederik P Kingma, Abhishek Kumar, Stefano Ermon, and Ben Poole. Score-based generative modeling through stochastic differential equations. *arXiv preprint arXiv:2011.13456*, 2020.
- [26] Yang Song and Stefano Ermon. Generative modeling by estimating gradients of the data distribution. *Advances in neural information processing systems*, 32, 2019.
- [27] Omri Avrahami, Dani Lischinski, and Ohad Fried. Blended diffusion for text-driven editing of natural images. In *Proceedings of the IEEE/CVF Conference on Computer Vision and Pattern Recognition*, pages 18208–18218, 2022.
- [28] Aditya Ramesh, Prafulla Dhariwal, Alex Nichol, Casey Chu, and Mark Chen. Hierarchical text-conditional image generation with clip latents. *arXiv preprint arXiv:2204.06125*, 2022.
- [29] Shuyang Gu, Dong Chen, Jianmin Bao, Fang Wen, Bo Zhang, Dongdong Chen, Lu Yuan, and Baining Guo. Vector quantized diffusion model for text-to-image synthesis. In *Proceedings of the IEEE/CVF Conference on Computer Vision and Pattern Recognition*, pages 10696–10706, 2022.
- [30] Alex Nichol, Prafulla Dhariwal, Aditya Ramesh, Pranav Shyam, Pamela Mishkin, Bob McGrew, Ilya Sutskever, and Mark Chen. Glide: Towards photorealistic image generation and editing with text-guided diffusion models. *arXiv preprint arXiv:2112.10741*, 2021.
- [31] Jonathan Ho, Tim Salimans, Alexey Gritsenko, William Chan, Mohammad Norouzi, and David J Fleet. Video diffusion models. *arXiv preprint arXiv:2204.03458*, 2022.
- [32] Uriel Singer, Adam Polyak, Thomas Hayes, Xi Yin, Jie An, Songyang Zhang, Qiyuan Hu, Harry Yang, Oron Ashual, Oran Gafni, et al. Make-a-video: Text-to-video generation without text-video data. *arXiv preprint arXiv:2209.14792*, 2022.
- [33] Nataniel Ruiz, Yuanzhen Li, Varun Jampani, Yael Pritch, Michael Rubinstein, and Kfir Aberman. Dreambooth: Fine tuning text-to-image diffusion models for subject-driven generation. *arXiv preprint arXiv:2208.12242*, 2022.
- [34] Chitwan Saharia, William Chan, Saurabh Saxena, Lala Li, Jay Whang, Emily L Denton, Kamyar Ghasemipour, Raphael Gontijo Lopes, Burcu Karagol Ayan, Tim Salimans, et al. Photorealistic text-to-image diffusion models with deep language understanding. *Advances in Neural Information Processing Systems*, 35:36479–36494, 2022.

- [35] Jacob Austin, Daniel D Johnson, Jonathan Ho, Daniel Tarlow, and Rianne van den Berg. Structured denoising diffusion models in discrete state-spaces. *Advances in Neural Information Processing Systems*, 34:17981–17993, 2021.
- [36] Shansan Gong, Mukai Li, Jiangtao Feng, Zhiyong Wu, and LingPeng Kong. Diffuseq: Sequence to sequence text generation with diffusion models. *arXiv preprint arXiv:2210.08933*, 2022.
- [37] Xiang Li, John Thickstun, Ishaan Gulrajani, Percy S Liang, and Tatsunori B Hashimoto. Diffusion-lm improves controllable text generation. *Advances in Neural Information Processing Systems*, 35:4328–4343, 2022.
- [38] Ting Chen, Ruixiang Zhang, and Geoffrey Hinton. Analog bits: Generating discrete data using diffusion models with self-conditioning. *arXiv preprint arXiv:2208.04202*, 2022.
- [39] Vadim Popov, Ivan Vovk, Vladimir Gogoryan, Tasnima Sadekova, and Mikhail Kudinov. Grad-tts: A diffusion probabilistic model for text-to-speech. In *International Conference on Machine Learning*, pages 8599–8608. PMLR, 2021.
- [40] Junhyeok Lee and Seungu Han. Nu-wave: A diffusion probabilistic model for neural audio upsampling. *arXiv preprint arXiv:2104.02321*, 2021.
- [41] Nanxin Chen, Yu Zhang, Heiga Zen, Ron J Weiss, Mohammad Norouzi, and William Chan. Wavegrad: Estimating gradients for waveform generation. *arXiv preprint arXiv:2009.00713*, 2020.
- [42] Rongjie Huang, Zhou Zhao, Huadai Liu, Jinglin Liu, Chenye Cui, and Yi Ren. Prodiff: Progressive fast diffusion model for high-quality text-to-speech. In *Proceedings of the 30th ACM International Conference on Multimedia*, pages 2595–2605, 2022.
- [43] Robin Scheibler, Youna Ji, Soo-Whan Chung, Jaekyung Byun, Soyeon Choe, and Min-Seok Choi. Diffusion-based generative speech source separation. In *ICASSP 2023-2023 IEEE International Conference on Acoustics, Speech and Signal Processing (ICASSP)*, pages 1–5. IEEE, 2023.
- [44] Ludan Ruan, Yiyang Ma, Huan Yang, Huiguo He, Bei Liu, Jianlong Fu, Nicholas Jing Yuan, Qin Jin, and Baining Guo. Mm-diffusion: Learning multi-modal diffusion models for joint audio and video generation. *arXiv preprint arXiv:2212.09478*, 2022.
- [45] Tomer Amit, Tal Shaharabany, Eliya Nachmani, and Lior Wolf. Segdiff: Image segmentation with diffusion probabilistic models. *arXiv preprint arXiv:2112.00390*, 2021.
- [46] Dmitry Baranchuk, Ivan Rubachev, Andrey Voynov, Valentin Khruikov, and Artem Babenko. Label-efficient semantic segmentation with diffusion models. *arXiv preprint arXiv:2112.03126*, 2021.
- [47] Emmanuel Asiedu Brempong, Simon Kornblith, Ting Chen, Niki Parmar, Matthias Minderer, and Mohammad Norouzi. Denoising pretraining for semantic segmentation. In *Proceedings of the IEEE/CVF Conference on Computer Vision and Pattern Recognition*, pages 4175–4186, 2022.
- [48] Shoufa Chen, Peize Sun, Yibing Song, and Ping Luo. Diffusion-det: Diffusion model for object detection. *arXiv preprint arXiv:2211.09788*, 2022.
- [49] Olaf Ronneberger, Philipp Fischer, and Thomas Brox. U-net: Convolutional networks for biomedical image segmentation. In *Medical Image Computing and Computer-Assisted Intervention—MICCAI 2015: 18th International Conference, Munich, Germany, October 5-9, 2015, Proceedings, Part III 18*, pages 234–241. Springer, 2015.
- [50] Ashish Vaswani, Noam Shazeer, Niki Parmar, Jakob Uszkoreit, Llion Jones, Aidan N Gomez, Łukasz Kaiser, and Illia Polosukhin. Attention is all you need. *Advances in neural information processing systems*, 30, 2017.
- [51] Rui Qian, Di Hu, Heinrich Dinkel, Mengyue Wu, Ning Xu, and Weiyao Lin. Multiple sound sources localization from coarse to fine. In *European Conference on Computer Vision*, pages 292–308. Springer, 2020.
- [52] Yuxin Wu and Kaiming He. Group normalization. In *Proceedings of the European conference on computer vision (ECCV)*, pages 3–19, 2018.
- [53] Stefan Elfving, Eiji Uchibe, and Kenji Doya. Sigmoid-weighted linear units for neural network function approximation in reinforcement learning. *Neural Networks*, 107:3–11, 2018.

- [54] Vincent Dumoulin, Ethan Perez, Nathan Schucher, Florian Strub, Harm de Vries, Aaron Courville, and Yoshua Bengio. Feature-wise transformations. *Distill*, 3(7):e11, 2018.
- [55] Zhong-Qiu Wang, Samuele Cornell, Shukjae Choi, Younglo Lee, Byeong-Yeol Kim, and Shinji Watanabe. Tf-gridnet: Making time-frequency domain models great again for monaural speaker separation. In *ICASSP 2023-2023 IEEE International Conference on Acoustics, Speech and Signal Processing (ICASSP)*, pages 1–5. IEEE, 2023.
- [56] Kaiming He, Xiangyu Zhang, Shaoqing Ren, and Jian Sun. Deep residual learning for image recognition. In *Proceedings of the IEEE conference on computer vision and pattern recognition*, pages 770–778, 2016.
- [57] Reuben Tan, Arijit Ray, Andrea Burns, Bryan A. Plummer, Justin Salamon, Oriol Nieto, Bryan Russell, and Kate Saenko. Language-guided audio-visual source separation via trimodal consistency. 2023.
- [58] Colin Raffel, Brian McFee, Eric J Humphrey, Justin Salamon, Oriol Nieto, Dawen Liang, Daniel PW Ellis, and C Colin Raffel. Mir\_eval: A transparent implementation of common mir metrics. In *ISMIR*, pages 367–372, 2014.
- [59] Zhuoran Shen, Mingyuan Zhang, Haiyu Zhao, Shuai Yi, and Hongsheng Li. Efficient attention: Attention with linear complexities. In *Proceedings of the IEEE/CVF winter conference on applications of computer vision*, pages 3531–3539, 2021.